

Low cost electroluminescence lab implementation

Manoel Henrique de O. P. Filho and Vanuza Alves Teixeira¹

¹ Federal Institute of Education, Science and technology of Pernambuco, Campus Pesqueira, Pesqueira (Brazil)

Abstract

The electroluminescence (EL) test permits to obtain an image with active and inactive areas of photovoltaic (PV) solar cells. The occurrence of inactive areas is mainly caused by mechanical impact in PV module along its live steps; those areas cause efficiency and energy losses. This work presents the EL lab implementation with low-cost equipment such as a digital camera Sony cyber-shot DSC-WX9. The procedure to adapt the camera to get images of wave length near of PV cells emission is described in details. A low-power voltage sources suitable configured to inject short current (I_{sc}) values of PV modules was used. It was observed that, with this apparatus, the EL lab was properly implemented; it permitted to obtain pictures of EL PV cells emission with different PV module defects. A test with the relation ISO configurations vs percentage of I_{sc} injected was performed. The ISO 800 configuration of camera permits visually to detect inactive areas of cells in PV modules with values of injected electrical current less than 50 % of I_{sc} . This fact results in an even higher cost reduction with equipment.

Keywords: photovoltaic modules, electroluminescence test, microcrack solar cell.

1. Introduction

It's observed that with the installation of thousands of PV modules there's an initial necessity of skill work force formation for the equipment installation step. On other stage, it's noted that another type of skill is necessary to maintain and operate those power plants using different techniques of problem analysis with a suitable cost.

According to Mchedlidze *et al.* (2016), the PV modules performance degradation process is one of the things that concerns the most the community which uses these systems. The main degradation processes are fairly known: light induced degradation (LID), Potential Induced Degradation (PID), degradation related to impurities and structural defects in PV cells and in other parts of PV module, for instance, snail trails, anti-reflection coat degradation, glass transmittance and Ethylene Vinyl Acetate (EVA) degradation. These processes are expected by manufacturers that afford contractual warranties of performance for 25 years. Most manufacturers promise a mean performance degradation rate of 0.5% per year. This degradation rate is also used in long term PV power plant simulation for feasibility analysis and it's the maintenance staff job to monitor if the degradation level is upper or lower than those indicated by manufacturer.

This scenario can be changed when it's considered the human handling during almost all PV module life steps. Mechanical actions could happen with PV modules during transportation, storage, unpacking, installation and maintenance. Falling, shocks and mechanical efforts beyond the limits can produce micro cracks on solar cells (Figure 1b), because the PV cells have a very thin thickness, in order of 0.18 μm . Although the PV cells are encapsulated in PV module, they are sensitive to shocks (Jahn *et al.*, 2018). In those cases, only a EL test could point out the cracks, as presented in figures 1a and 1b. During all PV module life steps, the arise of micro cracks could result in the warranty activation of different services (conveyor, installer or maintenance).

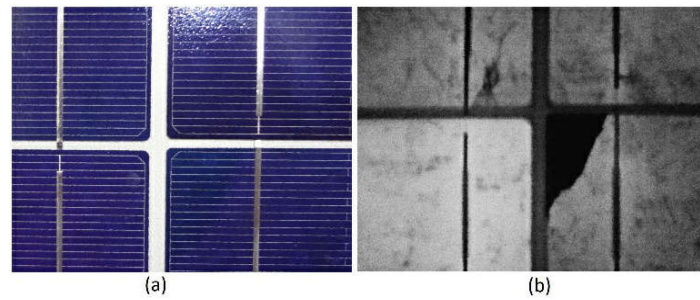


Fig. 1: a) PV solar cell visually without problems. b) EL emission image os the same PV cell with a cracked area.

Typical high-cost commercial solutions for EL images obtainment includes high performance cameras with voltage sources that inject the I_{sc} current in the PV module which are impracticable for tests on small or medium PV power plants. It's described, in this work, the EL low-cost lab implantation that uses a common digital camera (adapted for this purpose) and stand power sources. It's also reported the adaptation steps which made possible the obtainment of EL images by the digital camera previously mentioned. It was performed an evaluation of the electrical current value injected needed in the PV module versus the camera configuration, to get good quality images with less electrical current, lower than I_{sc} , that reduces the sources capacity needed for EL tests.

2. EL lab description

EL was the technique used to generate the images of figure 1. According to Abella (2016), it consists in the same principle of Light Emissive Diode (LED). It's injected an electrical current in the PV Cell or module, based on carrier radiative recombination; light is emitted with a spectral distribution as shown in figure 2.

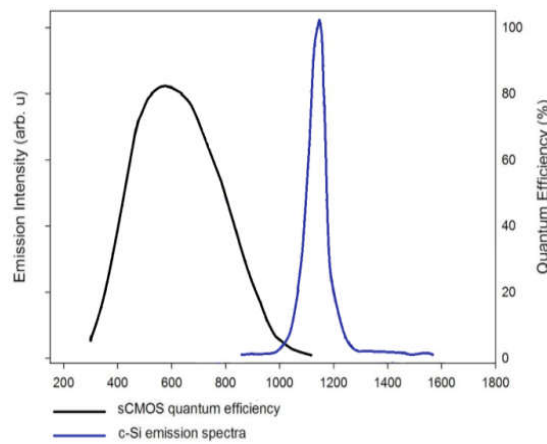


Fig. 2: Emission spectral from a range of crystalline silicon solar cell and the quantum. Adapted from Jahn *et al.* (2018).

The emission peak occurs with a wavelength distinct of visible light (400 – 700 nm). Special cameras are used with detectors that cover the spectral range (900 – 1300 nm) (electromagnetic spectra infrared range) indicated in figure 2 (Frazão, 2016). An example is the Canon EOS M3 - PV vision EL that has a spectral range around 1100 nm. Photos like the one shown in figure 1b are taken with this kind of equipment, but they're expensive; close to US\$ 6,100 (Bedin *et al.*, 2018).



Fig. 3: Camera Cyber-Shot DSC-WX9

The digital camera cyber-shot DSC-WX9 (Figure 3) was used in this work. Its resolution is 16.2 megapixels, with a CMOS image sensor, f2.6 of maximum diafrag aperture and the maximum speed of obturator 1/1600s. The DSC-WX9 has a Carl Zeiss Vario-Tessar lens with optical zoom of 5x. The sensibility of its image sensor (ISO) ranges from 100 to 3200.

The camera adaptation process consists on remove the infrared block filter from its image sensor to allow the cell emission reach the CMOS sensor thereby to permit the EL tests. The procedure for its adaptation should be executed very carefully to avoid damages to the camera.

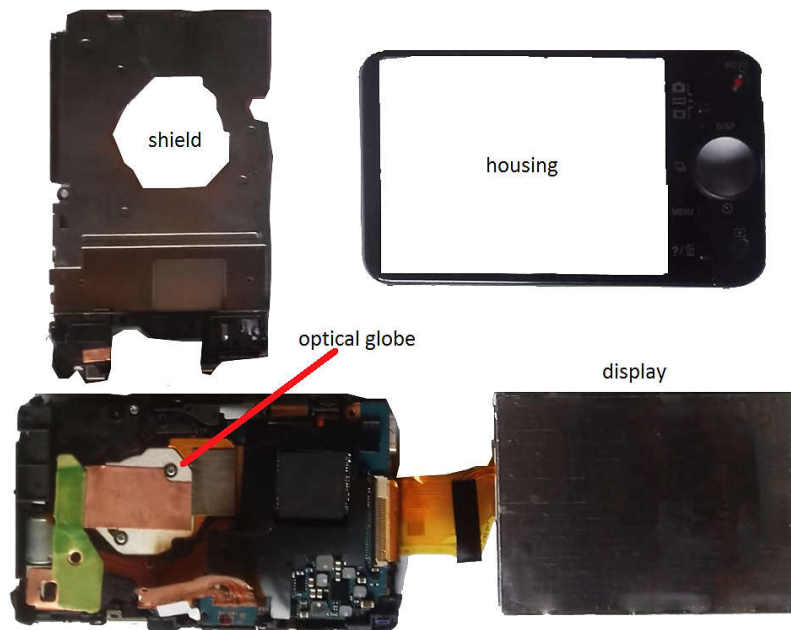


Fig. 4: Open camera showing the housing, the shield, the undocked display and the optical globe still mounted.

Initially, it was used a philips precision screwdriver (PH00-2mm) to remove the external screws permitting to withdraw the housing, that its divided in three parts (back, front and top) to access its internal parts (figure 4). After that, the user interface (little board with buttons) and the LCD screen (display) are shifted. Then, the shield and the screws that fix the optical sensor behind the Cyber-Shot optical set can be removed. The last step is unstick the block filter that is under the image sensor with a precision screwdriver of 1 mm (figure 5).



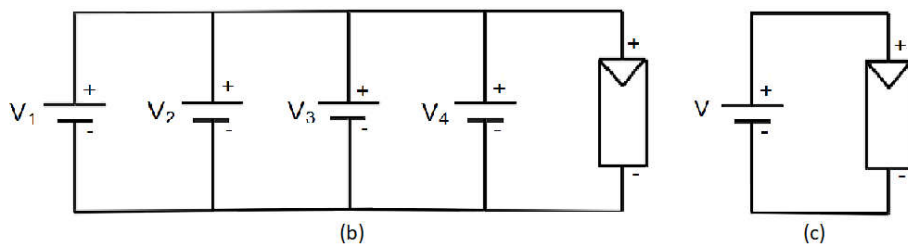
Fig. 5: Optical globe dosked with the filter removed (blue part).

The figure 5 presents the optical filter (in blue) and the sensor without it (red arrow). After ending the procedure described, all parts of DSC-WX9 must be assembled; after that, the camera will be able to take EL photos of PV modules.

According to Petraglia and Nardone (2011), the EL test must be done injecting electrical current in the PV module positive terminal. It was used the voltage sources Minipa model MPL-3303M (two independent sources of 32 V and 3 A) (figure 6a); this equipment could be configured in maximum as one source of 64 V and 3 A. The PV modules tested were a 50 Wp ($I_{sc} = 3.04$ A and $V_{oc} = 21.56$ V) and a 255 Wp ($I_{sc} = 9.01$ A and $V_{oc} = 37.7$ V). Four voltage sources were connected to supply suitable values of voltage and current. For instance, the test of 50 Wp module used only one source (figure 6c) and for the 255 Wp test, four power sources were connected in parallel (figure 6b).



(a)



(b)

(c)

Fig. 6: a) Four power sources configured in serial mode and connected in parallel, b) Electrical circuit relative to this configuration, c) Electrical circuit with one power source configured in independent mode.

3. Results

As initial assignment of EL lab implantation, EL images were taken of various PV modules installed inside and outside the lab. Some defects were detected such as broken solar cell, impure materials, etc (figure 7) and will be described in this chapter.

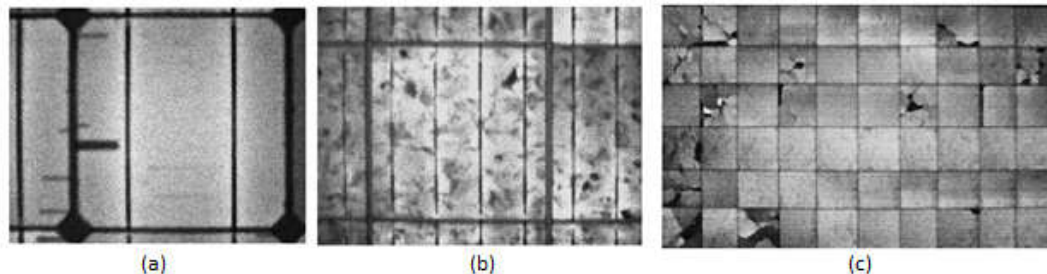


Fig. 7: a) PV cell with front contact interruption, b) impurities and c) module with broken PV cells.

All images in figure 7 were treated with a image processing software. The figure 7a shows monocrystalline PV cells submitted to a 2.8 A (approximately 50% of I_{sc}) that presents defects known as front contact interruptions. It occurs generally during the manufacturing cell process or cell assembly in module. Depending on the position and the interruption depth, the result of this defect in the PV module output power can vary a lot (Zettl *et al.*, 2012).

The EL images of some polycrystalline silicon PV modules presented imperfections with dark areas with granular aspect as shown in figure 7b The degradation process may be related to several factors including: fluctuations related to dopant concentration, thickness of cell material and the material quality itself. It is called silicon crystals heterogeneities; this type of defect can lead the PV cell to a less efficiency performance (Zettl *et al.*, 2012).

Cracks and disruptions of semiconductor materials are responsible for the majority of energy loss cases in crystalline silicon PV cells. The fissures generally propagate parallel to the module contact fingers. In some cases, they can disseminate perpendicular to the contact fingers, causing damage to them (Zettl *et al.*, 2012). The figure 7c, that is a module tested with 9 A (I_{sc}), shows the typical appearance of a module with broken cells, in this case, caused by a fall from a rooftop during its installation.

It was observed, after some tests, that the camera configuration could be changed, because some of the images were overshadowed. It was performed a test with a PV module with micro cracks comparing all configurations and the values of injected current. The figure 8 presents the results of four configuration possibilities and the fraction of I_{sc} current injected. The pictures in the figure 8 were not treated at all.

The Cyber-Shot DSC-WX9 has three modes of configuration: night mode, ISO mode (automatic) and auto programmed (ISO manually chosen, only ISO 800 and ISO 3200 were used). These four modes of test are compared against the fraction of I_{sc} and the results are shown in figure 8.

In night mode configuration, it's observed that with any value of injected electrical current, the visual detection of defects is difficult. In ISO mode (automatic), only with 100% of short circuit current is possible to visualize all defects, with 75% of I_{sc} is likely to identify some defect, although with impaired focus.

In the auto programmed mode (ISO 800), the pictures are more sharp, even with 50% of I_{sc} , and the defects can be identified easily. In the auto programmed mode (ISO 3200), it's observed that with 100% of I_{sc} , the image is saturated, covering up the module defects. In this configuration and with 25% of I_{sc} , it is possible to identify defects in better quality than the ISO mode (automatic) with 100% of I_{sc} .

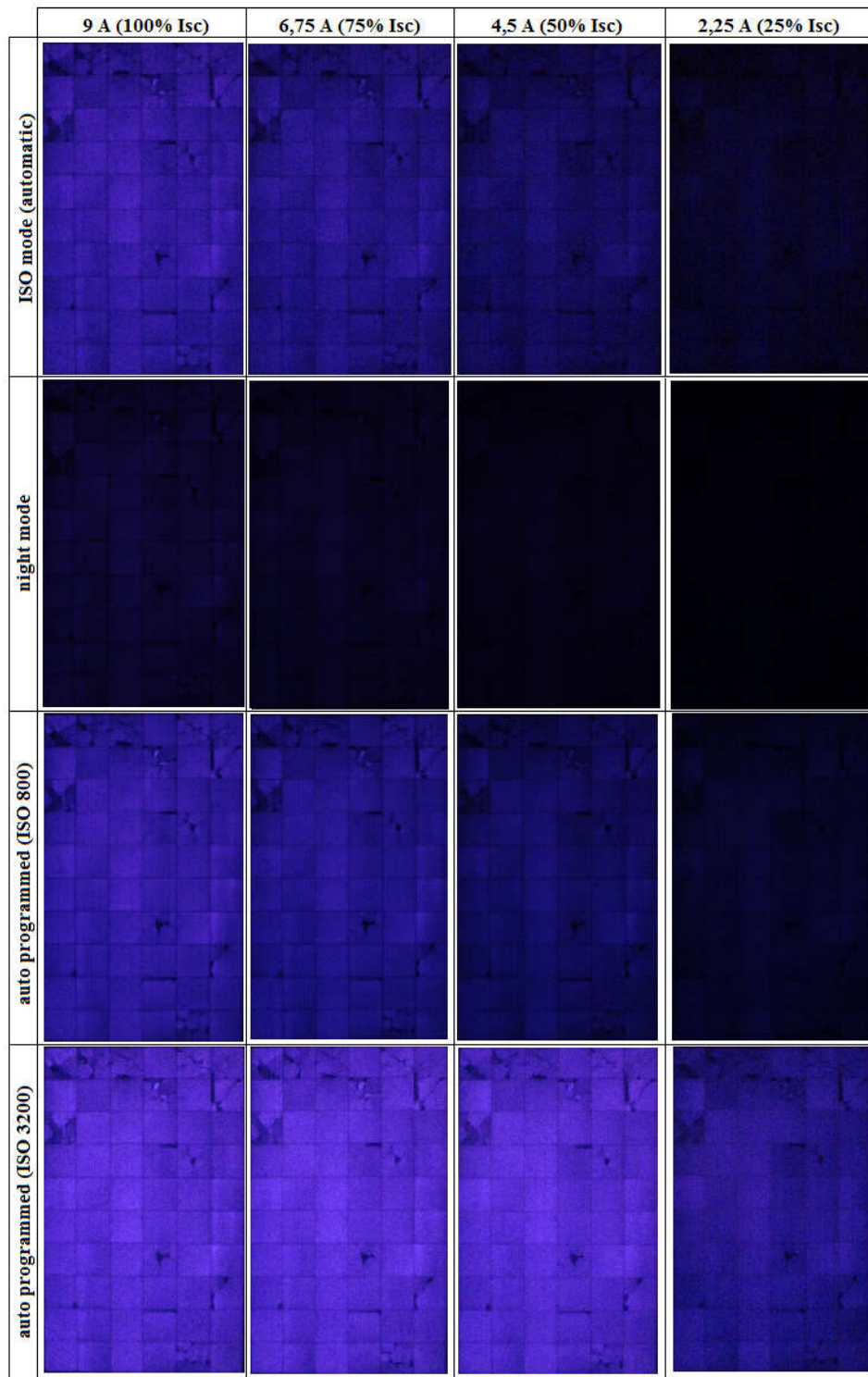


Fig. 8: Comparative of four camera configurations and four values of Isc fraction of injected current.

4. Conclusions

It was demonstrated with this work that it is possible to use common stand power source and a low cost digital camera (DSC-WX9) to realize EL tests. In order to achieve that, some adaptations and conexions must be made, as described. Using these equipments and after some tests, it was concluded that, depending on the camera configuration chosen, it is possible to define an adequate relation between exposition (ISO) and a fraction of I_{sc} injected in the PV module that allows to visualize and identify PV modules defects. Using, then, a low capacity current source than the nominal module I_{sc} , reduce significantly the tests costs of this technique implementation in lab as well as in field.

5. References

- Abella, M.A., 2016. Evaluación y Mantenimiento de centrales fotovoltaicas. Proceedings CIEMAT (Ed).
- Bedin, Caroline, Oliveira, Aline Kirten Vidal de, Nascimento, Lucas Rafael, Pinto, Gustavo Xavier de Andreade, Sergio, Lucas Augusto Zanicoski, R  ther, Ricardo, 2018. PID Detection in crystalline silicon modules using low-cost electroluminescence images in the field, Asia Pacific Solar Research Conference, Sydney.
- Fraz  o, M.S., 2016. Eletroluminesc  ncia de c  lulas solares. Energy, Geophysics and Geografy Engineering Department. Lisbon University.
- Jahn, U., Hera, M., K  ntges, M., Parlevliet, D., Paggi, M., 2018. Review on infrared and electroluminescence imaging for PV field applications. Proceedings Report IEA-PVPS T13-10, International Energy Agency .
- Mchedlidze, T., Herguth, A., Weber, J., 2016. Monitoring of Si-solar cell degradation with electroluminescence. Sol Energ Mat Sol C 155 38-42.
- Petraglia, A., Nardone, V., 2011. Electroluminescence in photovoltaic cell. Physics Education 46.
- Zettl, M., Mayer, O., Lynass, M., Bucher, M., Stern, O., Heller, C. and Mueggenburg, E., 2012. Defect detection in photovoltaic modules using electroluminescence imaging. 27th European Photovoltaic Solar Energy Conference and Exhibition, pp. 3374 – 3378.